

Supporting Information For

Double Layer Capacitance at Ionic Liquid – Boron Doped Diamond Electrode Interfaces  
Studied by Fourier Transformed Alternating Current Voltammetry

Anthony J. Lucio,<sup>1</sup> Scott K. Shaw,<sup>1\*</sup> Jie Zhang,<sup>2</sup> and Alan M. Bond<sup>2</sup>

<sup>1</sup>Department of Chemistry, University of Iowa, Iowa City, Iowa 52242, United States

<sup>2</sup>School of Chemistry, Monash University, Clayton, Victoria 3800, Australia

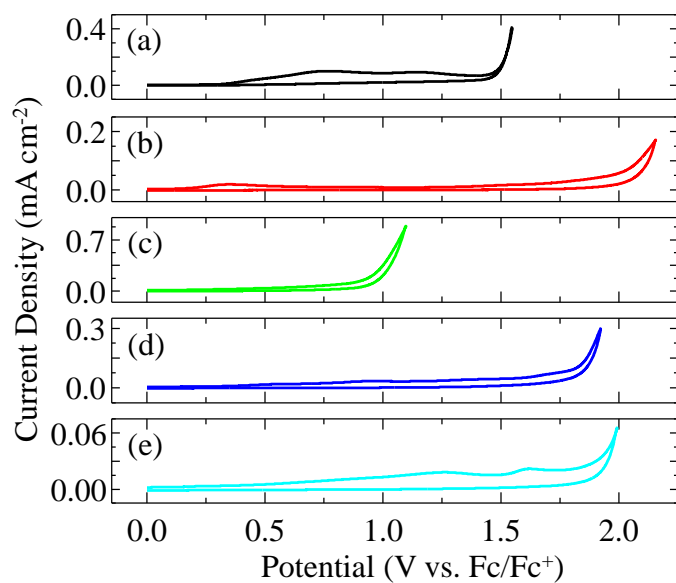


Figure S1. Zoomed in region near anodic potential limit from data in Figure 1 from use of a BDD electrode with (a) PAN, (b) N<sub>H222</sub> TFSI, (c) Bmim MeSO<sub>4</sub>, and (d) Bmim BF<sub>4</sub>, and (e) Bmim PF<sub>6</sub> on BDD. The DC scan rate is 100 mV s<sup>-1</sup>.

IL	$E_{\text{cathodic}}$ (V vs. Fc/Fc <sup>+</sup> )	$E_{\text{anodic}}$ (V vs. Fc/Fc <sup>+</sup> )	$E_{\text{total}}$ (V)
PAN	-1.7	+1.5	3.2
N <sub>H222</sub> TFSI	-2.2	+2.0	4.2
Bmim MeSO <sub>4</sub>	-2.7	+1.0	3.7
Bmim BF <sub>4</sub>	-2.7	+1.8	4.5
Bmim PF <sub>6</sub>	-2.5	+1.9	4.4

Table S1. Cathodic ( $E_{\text{cathodic}}$ ) and anodic ( $E_{\text{anodic}}$ ) potential limits versus the reversible potential for Fc/Fc<sup>+</sup> and the potential window ( $E_{\text{total}}$ ) available in the ILs with a BDD electrode.

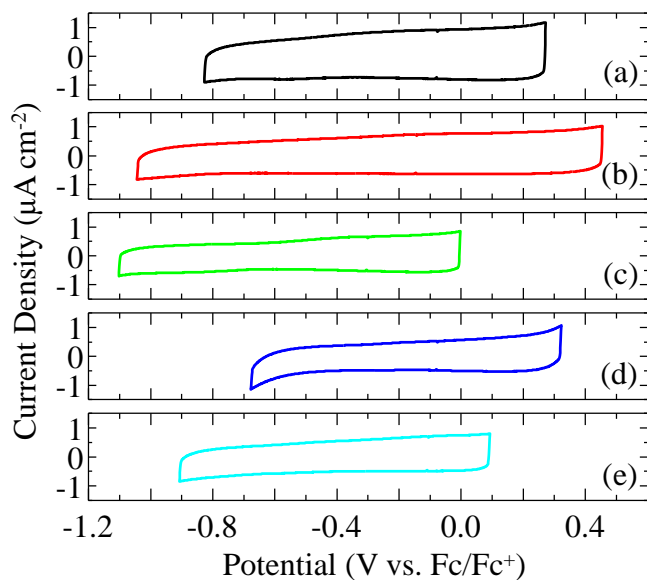


Figure S2. DC CVs within the selected double layer window for a BDD electrode in (a) PAN, (b)  $N_{H222}$  TFSI, (c) Bmim  $MeSO_4$ , and (d) Bmim  $BF_4$ , and (e) Bmim  $PF_6$  on BDD. The DC scan rate is  $100\text{ mV s}^{-1}$ .

## SI Discussion:

FT-ACV provides many details of the EDL response from a single experiment. **Figure S3** shows the total current (DC plus AC) data for each of the five ILs using a sine wave perturbation of 9 Hz with an amplitude of 80 mV. The initial (positive) potential scan direction is illustrated from  $t = 0$  to 27 s, while the return (negative) potential scan direction is shown from  $t = 27$  to 54 s. The total current data are relatively featureless and symmetric about the switching potential ( $t = 27$  s). Use of the Fourier transform allows the time-domain data to be converted into the frequency-domain to give the power spectra displayed in **Figure S4** with the major contributor being the fundamental harmonic component at 9 Hz. A small contribution arises from the aperiodic DC component at ca. 0 Hz. A very small second harmonic component at 18 Hz is assigned to minor deviations from an ideal capacitor. **Figure S5** provides the magnitudes of the fundamental through fifth harmonic components for a BDD electrode in PAN after band selection and inverse Fourier transformation of the data contained in the power spectrum. The third harmonic is close to zero and no fourth or fifth harmonic signal is detected.

Overall, large fundamental harmonic components are observed with minimal to unmeasurable second and higher order harmonics. This implies a nearly exclusive capacitive current response over the potential region considered. The uncompensated resistance values show negligible variation with potential in the potential ranges examined here. The electrochemical cell time constants (i.e.  $\tau = RC$ ) from our FT-ACV measurements are on the order of milliseconds. These metrics demonstrate the electrochemical systems examined in the present work is behaving similar to an ideal capacitor. This justifies the use of a simple RC circuit to model the data.

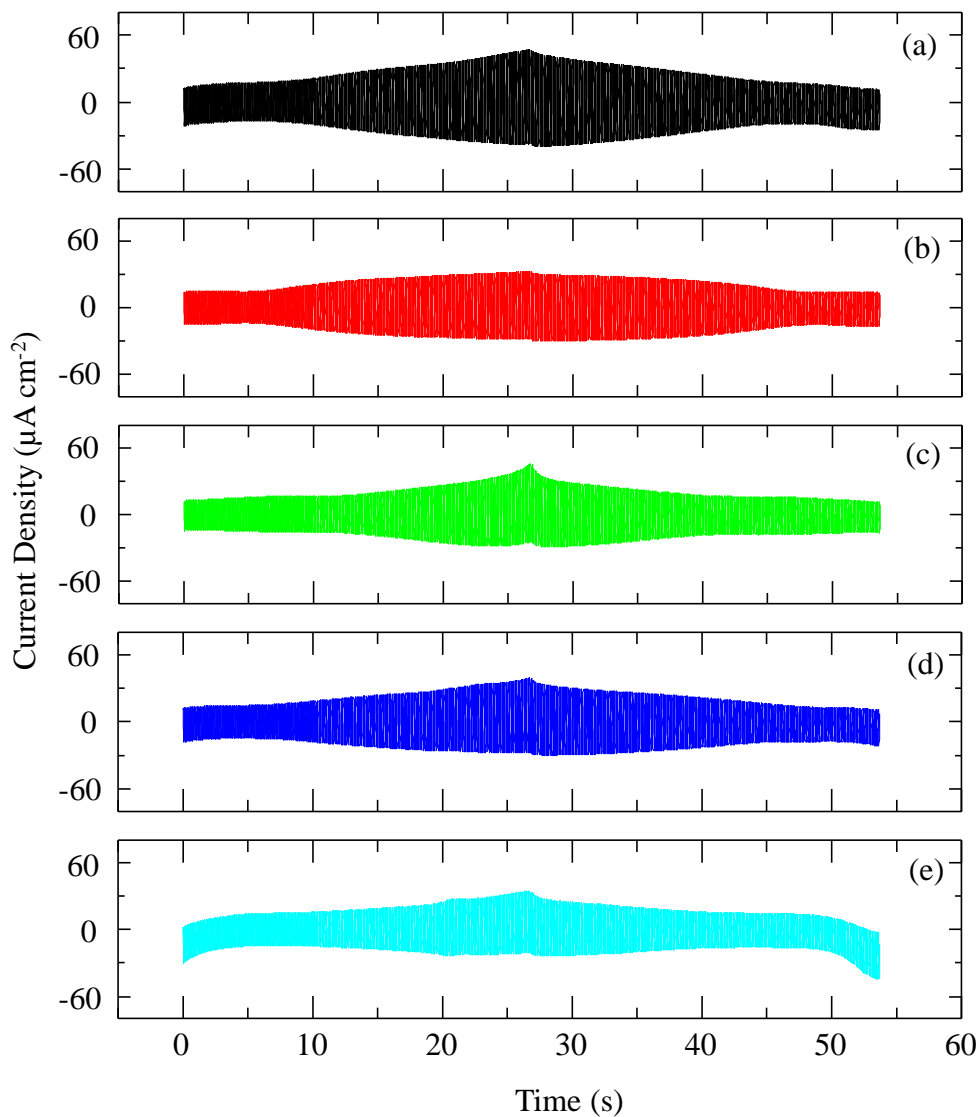


Figure S3. Total current (AC plus DC) versus time data obtained at a BDD electrode in (a) PAN with  $v = 78.20 \text{ mV s}^{-1}$ ,  $E_{\text{initial}} = -1.33 \text{ V}$ ,  $E_{\text{switch}} = +0.77 \text{ V}$ , (b)  $\text{N}_{\text{H222}}$  TFSI with  $v = 93.10 \text{ mV s}^{-1}$ ,  $E_{\text{initial}} = -1.55 \text{ V}$ ,  $E_{\text{switch}} = +0.95 \text{ V}$ , (c) Bmim  $\text{MeSO}_4$  with  $v = 78.20 \text{ mV s}^{-1}$ ,  $E_{\text{initial}} = -1.60 \text{ V}$ ,  $E_{\text{switch}} = +0.50 \text{ V}$ , (d) Bmim  $\text{BF}_4$  with  $v = 74.50 \text{ mV s}^{-1}$ ,  $E_{\text{initial}} = -1.18 \text{ V}$ ,  $E_{\text{switch}} = +0.82 \text{ V}$ , and (e) Bmim  $\text{PF}_6$  with  $v = 74.50 \text{ mV s}^{-1}$ ,  $E_{\text{initial}} = -1.40 \text{ V}$ ,  $E_{\text{switch}} = +0.60 \text{ V}$ . Potentials are versus  $\text{Fc}/\text{Fc}^+$  reference scale.  $\Delta E_{\text{amp}} = 80 \text{ mV}$ ,  $f = 9 \text{ Hz}$ .

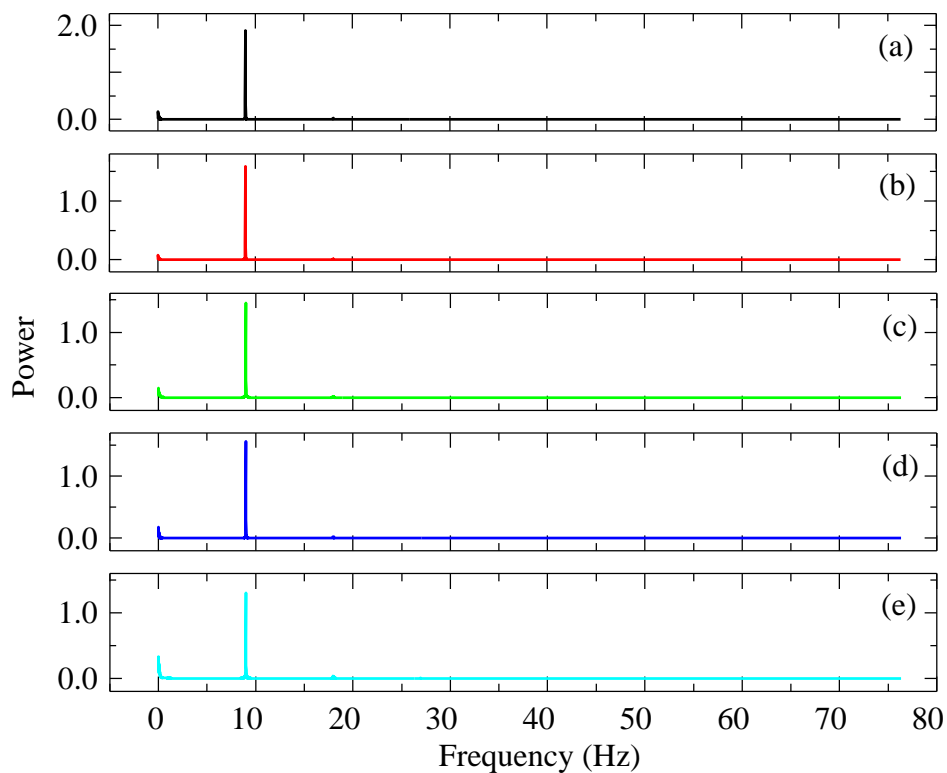


Figure S4. Power spectra derived from data in Figure S1 from use of a BDD electrode with (a) PAN, (b)  $N_{H222}$  TFSI, (c) Bmim MeSO<sub>4</sub>, and (d) Bmim BF<sub>4</sub>, and (e) Bmim PF<sub>6</sub> on BDD.

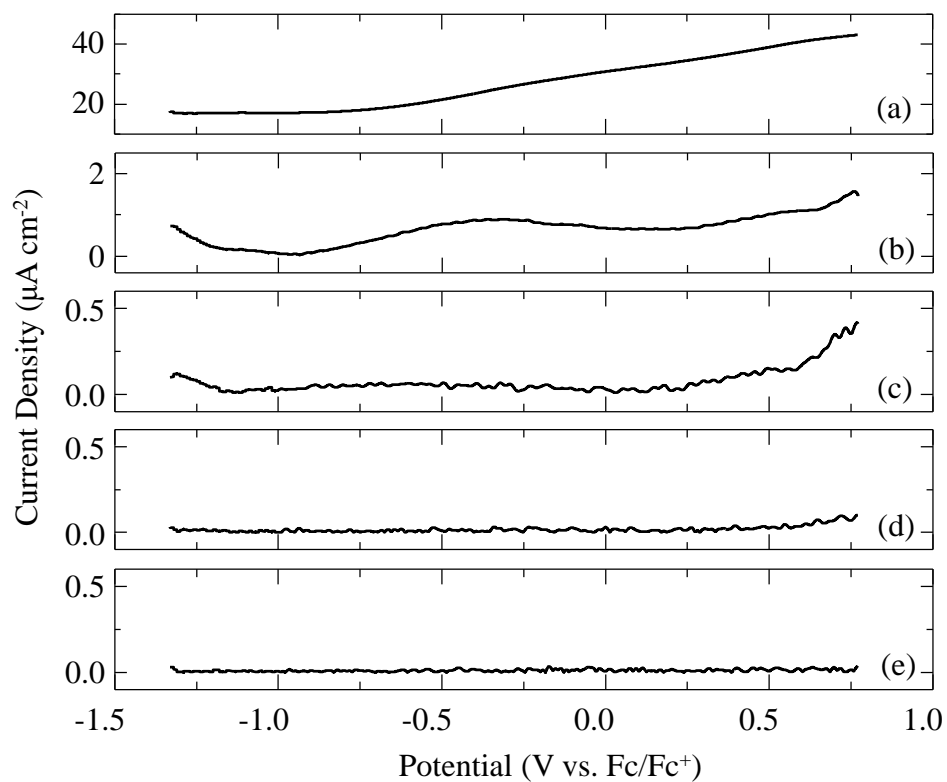


Figure S5. Representative plot of the (a) first, (b) second, (c) third, (d) fourth and (e) fifth AC harmonic components derived from FT-ACV measurements for PAN at a BDD electrode.  $\Delta E_{\text{amp}} = 80 \text{ mV}$ ,  $f = 9 \text{ Hz}$ , and  $v = 78.20 \text{ mV s}^{-1}$ .



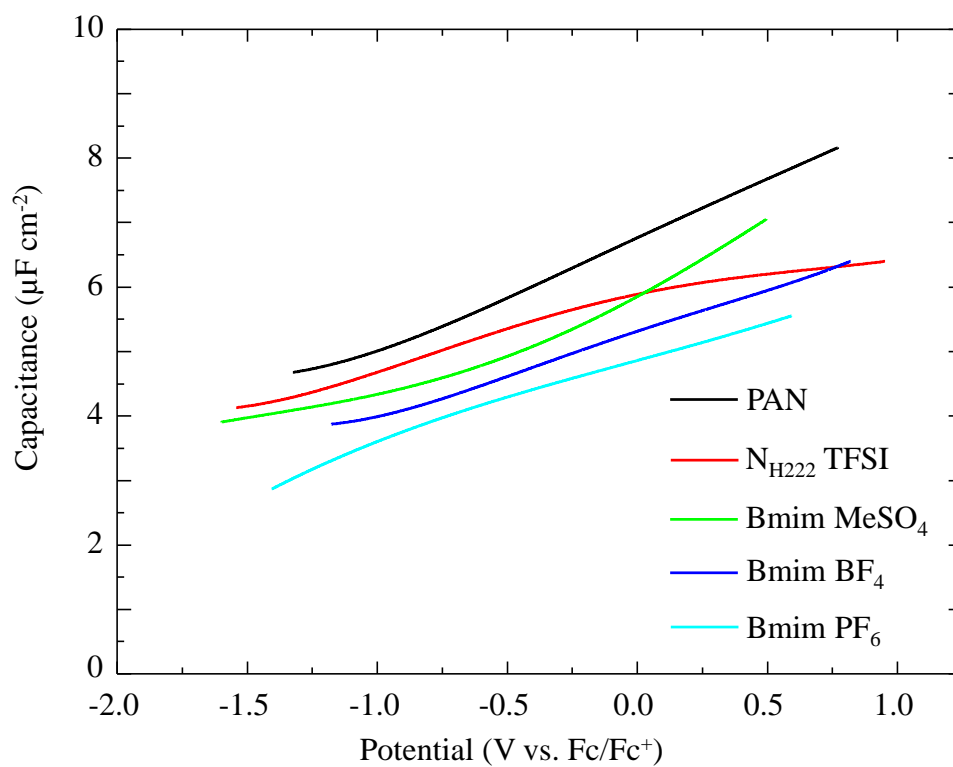


Figure S6. Overlay of capacitance versus potential data generated from the FT-ACV fundamental harmonic data using equation 1 for the five ILs in this study  $\Delta E_{\text{amp}} = 80 \text{ mV}$ ,  $f = 9 \text{ Hz}$ .